

1
2
3
4
5
6
7
8
9
10
11

Ambient Air Pollution Exposure Estimation for the Global Burden of Disease 2013

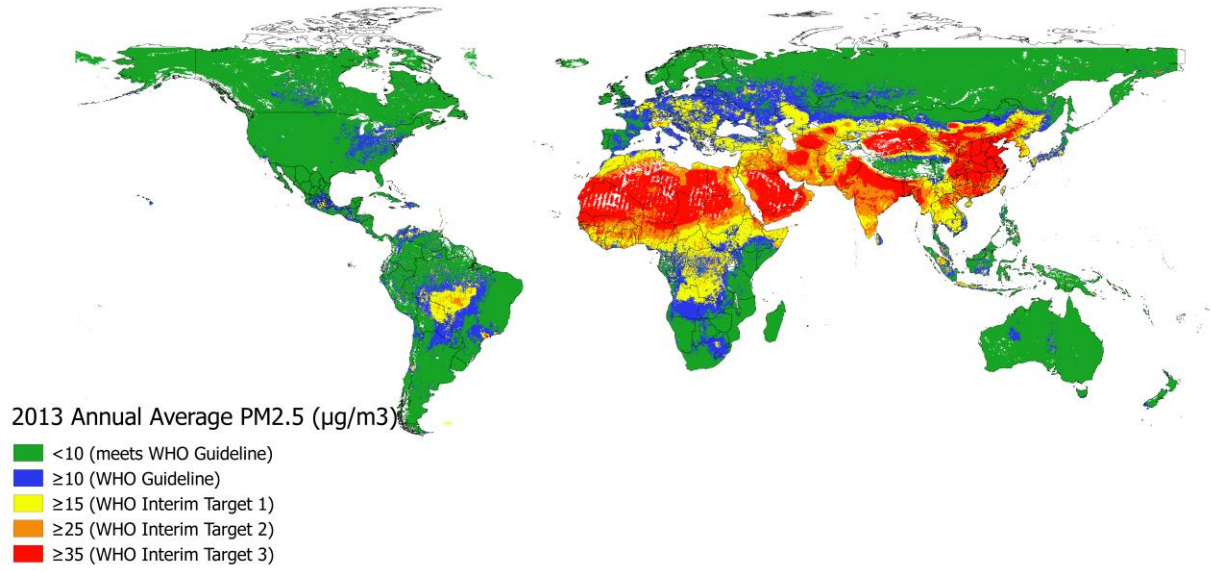
To be submitted to Environmental Science and Technology

12 **Abstract**

13 Exposure to ambient air pollution is a major risk factor for global disease. Assessment of the
14 impacts of air pollution on population health and the evaluation of trends relative to other major
15 risk factors requires regularly updated, accurate, spatially resolved exposure estimates. We
16 combined satellite-based estimates, chemical transport model (CTM) simulations and ground
17 measurements from 79 different countries to produce new global estimates of annual average
18 fine particle (PM_{2.5}) and ozone concentrations at 0.1° × 0.1° spatial resolution for five-year
19 intervals from 1990-2010 and the year 2013. These estimates were then applied to assess
20 population-weighted mean concentrations for 1990 – 2013 for each of 188 countries. In 2013,
21 87% of the world’s population lived in areas exceeding the World Health Organization (WHO)
22 Air Quality Guideline of 10 µg/m³ PM_{2.5} (annual average). Between 1990 and 2013, decreases in
23 population-weighted mean concentrations of PM_{2.5} were evident in most high income countries,
24 in contrast to increases estimated in South Asia, throughout much of Southeast Asia, and in
25 China. Population-weighted mean concentrations of ozone increased in most countries from
26 1990 - 2013, with modest decreases in North America, parts of Europe, and several countries in
27 Southeast Asia.

28

29 TOC Art



30

31

32

33 **Introduction**

34 The Global Burden of Disease (GBD) 2010 provided important new estimates of the global
35 health impacts attributable to ambient air pollution. Ambient particulate matter air pollution
36 (PM_{2.5}, particulate matter with aerodynamic diameter 2.5 μm or smaller) was identified as a
37 leading risk factor for global disease burden with an estimated 3.2 million attributable deaths in
38 the year 2010. An additional 152,000 deaths in 2010 were attributable to long term exposure to
39 ozone¹. These two pollutants were selected as indicators of exposure to ambient air pollution
40 based on extensive epidemiologic and mechanistic evidence indicating independent adverse
41 health impacts². These disease burden estimates incorporated novel high resolution global air
42 pollution exposure estimates for 1990, 2005, and 2010 that included both urban and rural areas
43 and that merged data from ground measurements, satellite retrievals and chemical transport
44 models. In addition to the application of these exposure estimates to the entire global population,
45 their high spatial resolution minimized biases due to spatial misalignment between exposure to
46 air pollution and population information³. Beyond their direct use in the GBD 2010, the PM_{2.5}
47 exposure estimates were combined with chemical transport model simulations to estimate the
48 sector-specific contributions to disease burden from motor vehicle transportation^{4,5}, household
49 cooking with solid fuels⁶ and household heating⁷. Additionally, these exposure estimates served
50 as the basis of the World Health Organization (WHO) air pollution mortality estimates⁸ and were
51 used by the World Bank as indicators of sustainable development⁹ and to estimate the economic
52 damages attributable to air pollution¹⁰. The estimates have also been used in the U.S.
53 Environmental Protection Agency's (USEPA) BenMap tool¹¹ which allows users to estimate
54 health impacts and economic value of changes in air quality, and figured prominently in the
55 exposure description of the International Agency for Research on Cancer Monograph on the

56 carcinogenicity of outdoor air pollution¹². Given the lack of ground measurements in many
57 regions of the world, the above analyses were not previously possible prior to development of
58 consistent, globally applicable exposure estimates.

59
60 In the context of the most recent update of the Global Burden of Disease (GBD 2013)¹³ we
61 developed updates and revised global exposure estimates for PM_{2.5} and ozone (O₃) with specific
62 emphasis on evaluation of trends between 1990 – 2013. We also incorporated improvements in
63 satellite-based estimation of PM_{2.5}¹⁴, the availability of internally consistent emissions
64 inventories spanning this entire period and a substantially increased number of ground
65 measurements of particulate matter, compared to those utilized previously. Here we describe the
66 methodology, provide descriptive information on year 2013 air pollution concentrations and
67 illustrate trends since 1990, at the country level.

68

69 **Methods**

70 *PM_{2.5}*

71 The overall approach taken to estimate annual average PM_{2.5} concentrations uses the mean of
72 gridded values of satellite-based and chemical transport model estimates, calibrated to available
73 ground measurements. In the previous GBD (2010) we used satellite-based estimates for PM_{2.5}
74 for the year 2005¹⁵ combined with simulations from the TM5 (Tracer Model, version 5) chemical
75 transport model¹⁶ based on year 2005 emissions, which were the most current update available at
76 the time of analysis. To estimate exposures for 1990 we used a TM5 simulation based on 1990
77 emissions but with the same “standard” meteorology as in the 2005 simulation. For the 1990

78 satellite-based estimates we used the same spatial pattern from the year 2005 estimates and
79 adjusted this to 1990 based upon the ratio of 2005:1990 simulations from the GEOS-Chem
80 chemical transport model¹⁷ that used anthropogenic emissions from these years (while again
81 maintaining consistent meteorology and natural emissions). For year 2010 estimates, we used the
82 2005 TM5 and satellite-based estimates and extrapolated these to 2010 based on the 1990 – 2005
83 trend following an assumption that the change proportional to the time period length from 2005
84 to 2010, relative to 2005 was 1/3 as large as the change from 1990 to 2005, relative to 1990 as
85 described by the formula:

$$86 \quad (PM_{2.5_2010} - PM_{2.5_2005}) / PM_{2.5_2005} = 1/3 * (PM_{2.5_2005} - PM_{2.5_1990}) / PM_{2.5_1990}. \quad (1)$$

87 In addition, we compiled available $PM_{2.5}$ (and where no $PM_{2.5}$ measurements were available,
88 PM_{10}) annual average measurement data for ~2005 from a variety of sources². These
89 measurements were used to calibrate the average of the TM5 and satellite-based estimates for
90 2005 at the $0.1^\circ \times 0.1^\circ$ grid-cell resolution with a simple prediction equation based upon
91 agreement between the average of TM5 and satellite-based estimates for those locations with
92 measurements.

93 For GBD 2013, we followed a similar approach but used updated inputs. Specifically, we used a
94 new series of satellite-based estimates for $PM_{2.5}$ that included year-specific (3 year averages of
95 retrievals centered on the specific year of interest) estimates for 1998 – 2012 and an improved
96 estimation algorithm¹⁴. Briefly, satellite-based $PM_{2.5}$ estimates used aerosol optical depth
97 (AOD) retrievals from satellites to estimate near-surface $PM_{2.5}$ by applying the relationship of
98 $PM_{2.5}$ to AOD simulated by the GEOS-Chem chemical transport model. These updated $PM_{2.5}$
99 estimates make use of both “unconstrained” (as used on GBD 2010) and “optimal-estimation”

100 AOD retrievals in combination with the MODIS¹⁸, MISR^{19,20} and SeaWiFS²¹ satellite-borne
101 instruments. In the optimal estimation approach, AOD retrievals using observed MODIS top-of-
102 atmosphere reflectance are constrained by simulated AOD based on their relative uncertainties.
103 The PM_{2.5} estimates produced by optimal estimation additionally used vertical profile
104 information from the CALIOP²² satellite instrument to inform about the relationship between
105 column AOD and ground-level concentrations. These two (optimal estimation and
106 unconstrained) sets of estimates were then combined with information on temporal variation
107 based on SeaWiFS and MISR to estimate global PM_{2.5} estimates (50% RH) at 0.1° x 0.1° for
108 2000, 2005, 2010 and 2011 (based on 3 years of retrievals, centered on the year of interest).
109 Estimates for 1995 and 1990 were based on the ratio of GEOS-Chem simulations that used
110 anthropogenic emissions (from EDGAR²³) between 2005 and the respective year of interest, but
111 constant meteorology²⁴.

112 We also included new TM5-FASST^{25,26} (FAst Scenario Screening Tool, a reduced-form version
113 of TM5) simulations for 1990, 2000, and 2010, using an updated set of emissions inventories,
114 and constant meteorological inputs and emissions from dust and sea salt. TM5-FASST is a
115 reduced form version of the TM5 chemical transport model that was used in the GBD 2010
116 exposure estimates. TM5 is a nested 3-dimensional global atmospheric chemistry transport
117 model, which simulates ozone and aerosol components at 1° x 1° resolution¹⁶. TM5 FASST
118 emulates the full TM5 chemical transport model with a set of linear relationships between
119 emissions in 56 geographically defined source regions, and pollutant concentrations in receptor
120 regions. TM5 FASST simulations are at a resolution of 1° x 1° grid cells that are sub-allocated
121 based on population density (using the Gridded Population of the World, version 3, GPWv3²⁷).
122 Here we used a consistent set of emissions estimates [ECLIPSE (IEA) 2010, 2000, 1990

123 emissions; RCP: international aviation and shipping (2010); GFED v3.1: Forest fires and
124 savannah burning (2000, 2010)] and “typical” (year 2001) meteorology, dust, and sea salt
125 contributions with TM5-FASST to simulate ambient (50% RH) PM_{2.5} concentrations at 0.1° x
126 0.1 ° for 1990, 2000 and 2010. Estimates for 1995 and 2005 were generated by fitting a natural
127 cubic spline to the 1990, 2000 and 2010 estimates. Estimates for 2011 were estimated by fitting
128 a natural spline to the 1990, 2000 and 2010 estimates, then extrapolating from the 2009 and 2010
129 fitted values. Full TM5 simulations for 1990 and 2005 (as used in GBD 2010) were also
130 available.

131 To collect updated measurement data for 2010-2013, we used a variety of information sources
132 including those used previously²⁸, as well as new data, especially from China and India, where
133 available. We sought input from an international group of GBD collaborators, conducted targeted
134 searches for data and included measurements compiled from a literature search¹⁴ and from the
135 WHO ambient air pollution in cities database⁸. A final database was constructed including
136 measurement values, year of annual average (2010-2013 data were targeted – other years were
137 used only if no other data were available), site coordinates (if available, or city centroid
138 coordinates if not available), site type (if available), iso3 country code, data source and whether
139 PM_{2.5} was measured directly or estimated from a PM_{2.5}:PM₁₀ ratio. All data sources are listed in
140 the Supporting Information. Given the spatial biases in availability of ground measurements,
141 differences in measurement approaches between jurisdictions, and absence of details regarding
142 measurement data in some instances, the ground measurements were not used in evaluation of
143 the exposure assessment methodology but rather incorporated within the approach as an
144 additional source of information. For locations where daily values were obtained or where
145 measurement completeness was available we retained all sites with >70% valid measurements,

146 as reported in the source databases. For locations where data were obtained for multiple years at
147 the same location we retained one value per location, between the years 2008-2013 in the
148 following order of preference: 2010, 2011, 2009, 2012, 2008, 2013 to best match the temporal
149 scale of the satellite-based and TM5-FASST estimates.

150 If multiple monitoring types available at the same site were included in parent databases, these
151 values were averaged. Industrial and roadside sites were excluded (where indicated in source
152 databases; except in India where these were retained upon the advice of local experts who
153 indicated that these sites adequately represent population exposure in that country). In the
154 USEPA database, sites indicated as "background surveillance" were designated as to
155 background, those indicated as "continuous air monitoring program", "population-oriented
156 monitoring", or "exposure studies" were designated as population sites. Those sites identified as
157 "episode monitoring" or "complaint investigation", were excluded. All others were identified as
158 unspecified and retained. Measurements flagged as "events," in the USEPA database were also
159 excluded.

160 In locations where no $PM_{2.5}$ measurements were available, we estimated $PM_{2.5}$ from
161 measurements of PM_{10} ^{2,29}. We preferentially used $PM_{2.5}:PM_{10}$ ratios that were locally derived. In
162 these cases ratios from any sites within 50 km where both PM_{10} and $PM_{2.5}$ were measured were
163 used to estimate $PM_{2.5}$ from PM_{10} measurements. These local ratios were only accepted and used
164 to derive $PM_{2.5}$ estimates for nearby sites if they were between 0.2 and 0.8. If local ratios were
165 not available we used a country and monitor-specific average if available, followed by a country-
166 specific average. Otherwise, we assumed a ratio of 0.5 to estimate $PM_{2.5}$ from PM_{10}
167 measurements.

168

169 In total we included 4073 data points from 3387 unique locations (1,854 [46%] from direct
170 measurements of PM_{2.5}) in 79 countries (Figure S1; Supporting Information). Of the 2219 data
171 points in which PM_{2.5} was estimated from PM₁₀, 1,151 (30% of 4073 total) were estimated using
172 a ratio derived from monitors within 50 km, 590 (15%) were estimated using in-country
173 monitors of the same type, and 309 (8%) were estimated with other in-country monitors. Finally,
174 the remaining 169 (4%) were estimated with a ratio of 0.5, as used for GBD 2010. The mean
175 ratio for the estimation was 0.61.

176 We then used a regression calibration approach to combine the mean of the satellite-based
177 estimates and the TM5-FASST simulations with the measurements to produce final global
178 estimates at 0.1° x 0.1° grid-cell resolution. For the regression calibration, we initially evaluated
179 a simple regression model:

$$180 \quad \text{Measured } \ln(\text{PM}_{2.5}) = \beta_0 + \beta_1 * \ln(\text{fused}) \quad (2)$$

181 where fused is the mean of the satellite-derived and TM5 estimates for each grid cell. We first
182 tested whether to apply a single global calibration function or one that varied by the 21 GBD
183 regions. Modeling with a random effect by 7 aggregated “super-regions” (due to the complete
184 absence of measurements in multiple regions) indicated some regional variation in slopes but
185 also some very poor fits in some regions, so a single global calibration function was chosen.
186 Evaluation of model residuals indicated no association with population density and addition of
187 population density to the model only minimally improved fit. We then evaluated the impact of
188 including available information on the measurement values and measurement sites including
189 whether the exact site coordinates were known, whether PM_{2.5} was directly measured or
190 estimated and whether the monitoring site classification was known or unspecified. Inclusion of

191 these variables slightly improved the model R^2 while slightly reducing the residual standard
192 error.

193 These two candidate global calibration models (Simple model: Intercept= 0.82, $\ln(\text{fused})= 0.73$,
194 residual standard error = 0.43, Multiple R-squared: 0.60, Adjusted R-squared: 0.60;
195 “Advanced” model with additional site parameters: Intercept= 0.42, $\ln(\text{fused})=0.87$, residual
196 standard error = 0.41, Multiple R-squared: 0.64, Adjusted R-squared: 0.64) were further
197 evaluated by a cross-validation procedure in which 10% of the measurement sites were randomly
198 selected for model evaluation. This procedure was repeated for a total of 3 separate sets of 10%
199 testing sites. In all cases the model with additional site parameters (“Advanced”, Figure S2;
200 Supporting Information) had a lower RMSE (12.17 vs 11.04; 12.17 vs 11.04; 10.21 vs 9.15) as
201 well as lower Akaike’s Information Criterion and Bayesian Information Criterion. Therefore, we
202 selected the model with additional site parameters that included variables to indicate approximate
203 location, unspecified monitor type, and $\text{PM}_{2.5}$ calculated from PM_{10} . A plot of these global
204 calibration functions against the data from ground measurements and the mean of the satellite-
205 based and TM5 estimates for the corresponding grid cells is provided in the Supporting
206 Information (Figure S2; Supporting Information). The relevant terms from this calibration
207 function were then used to adjust the gridded values of the mean of the satellite-based and TM5
208 estimates (“fused”) as follows:

$$209 \quad \text{Calibrated PM}_{2.5} = \exp[0.41765+(0.86953*\ln(\text{fused}))] \quad (3)$$

210 Estimates for 2013 were generated by extrapolating from the trend between the 2010 and 2011
211 fused and calibrated values. Specifically, for these extrapolations we assessed the rate of change

212 in concentrations between 2010 and 2011 and applied this growth rate to an exponential growth
213 function to estimates concentrations in 2013, with the following function:

$$214 \quad PM_{2.5_2013} = PM_{2.5_2010} * \exp(\text{rate.of.change} * (2013-2010)) \quad (4)$$

215 where, (annual) rate.of.change = $\ln(PM_{2.5_2011} / PM_{2.5_2010})$. The final $PM_{2.5}$ estimates used in
216 the burden of disease estimation and presented in the Results section are the fused, calibrated,
217 and (where applicable) extrapolated values. National level population-weighted mean and 95%
218 uncertainty interval concentrations were estimated by sampling 1000 fused grid cell
219 concentrations from each country in combination with the calibration parameters and the
220 standard error of the calibration function. These draws were then weighted by the corresponding
221 grid cell population value (using the Gridded Population of the World, version 3, GPWv3²⁷).

222 *Ozone*

223 As in GBD 2010, we calculated a running 3-month average (of daily 1 hour maximum values)
224 for each grid cell over a full year and selected the maximum of these values. This metric was
225 chosen to align with epidemiologic studies of chronic exposure which typically employ a
226 seasonal (summer) average, and to account for global variation in the timing of the ozone
227 (summer) season²⁸. As described above, these estimates were simulated with TM5-FASST at
228 $0.1^\circ \times 0.1^\circ$ for 1990, 2000 and 2010 using the same emissions datasets and meteorological inputs
229 as for the $PM_{2.5}$ simulations. Estimates for 1995, 2005, and 2011 were generated by fitting a
230 natural cubic spline in the same manner as described previously for $PM_{2.5}$. As described above
231 for $PM_{2.5}$, an exponential growth model for ozone concentrations was used to estimate 2013
232 concentrations from the 2011 estimates. Population weighted mean concentrations and 95%
233 uncertainty intervals for each country were estimated as described above for $PM_{2.5}$ and assuming

234 a normal distribution with a standard deviation calculated by assuming an uncertainty interval of \pm
235 6% of the estimated concentration. As in the GBD 2010 exposure estimates and given the scarcity
236 of surface ozone measurements throughout the world and the challenges in accessing hourly data
237 from available monitoring sites to develop the desired metric, we did not utilize surface ozone
238 measurements for developing the global estimates.

239

240 **Results**

241 Of the ground measurements, while 79 countries were represented, more than half were from
242 high income countries in North America (25%), Western (32%) and Central (12%) Europe.
243 Because of a major expansion of China's air quality monitoring network, 10% of the ground
244 measurements were from East Asia, and 5% were from South Asia. Countries in eleven regions
245 (Andean Latin America, Australasia, Central Asia, Eastern Europe, High-income Asia Pacific,
246 North Africa and Middle East, Southeast Asia, Southern Latin America, Southern Sub-Saharan
247 Africa, Tropical Latin America, Western Sub-Saharan Africa) each contributed less than 3% of
248 the measurement data, with no measurements at all from the other four regions (Caribbean,
249 Central Latin America, East and Central sub-Saharan Africa) of the world. The highest
250 measured annual average $PM_{2.5}$ concentration in the assembled measurement database was 194
251 $\mu g/m^3$ in Shijiazhuang, the capital of Hebei Province in China, while the lowest was $<1 \mu g/m^3$,
252 measured in Soldotna, Alaska, USA.

253 Year 2013 gridded estimates of annual average $PM_{2.5}$ and seasonal hourly maximum ozone
254 concentrations are displayed in Figures 1 and 2. The highest concentrations of $PM_{2.5}$ were
255 evident in northern Africa and the Middle East due to emissions of windblown mineral dust, and

256 in South and East Asia, especially in northern India and eastern China due to combustion
257 emissions from multiple sources including household solid fuel use, coal fired power plant
258 emissions, agricultural burning, industrial and transportation-related emissions. Ozone
259 concentrations were less variable spatially, but relatively higher in parts of the U.S., the Amazon
260 Basin, sub-Saharan Africa and throughout much of southern Europe, the Middle East and Asia.

261 The relationship between the spatial distribution of ambient concentrations and that of the
262 population is particularly relevant to health burden assessment (Figure 3). Based upon the grid-
263 cell concentration estimates and corresponding population data, 35% of global population
264 resided in areas with concentrations above the WHO Interim Target 1 of $35 \mu\text{g}/\text{m}^3$ annual
265 average $\text{PM}_{2.5}$ with nearly all of the most extreme ($> 65 \mu\text{g}/\text{m}^3$) concentrations experienced by
266 populations in China and India. Fully 87% of the global population resided in areas above the
267 WHO guideline of $10 \mu\text{g}/\text{m}^3$, with essentially none of the population of China (0.4%) or India
268 (0.01%) living in areas meeting this level.

269 Changes in estimated concentrations between 1990 and 2013 at the $0.1^\circ \times 0.1^\circ$ grid cell level are
270 shown in Figure 4. Large relative decreases were evident in the Eastern US., Europe, Russia and
271 in parts of Southeast Asia. In contrast, large relative increases were apparent in Western Canada,
272 parts of South America, the Middle East, India and China. Somewhat similar patterns were also
273 evident for ozone (Figure 5)

274 The trends in $\text{PM}_{2.5}$ are examined in more detail in Figures 6a-c which display population-
275 weighted mean (95% uncertainty interval) distributions of concentrations at the country level for
276 selected regions. Plots including all other countries are presented in the Supporting Information
277 (Figures S3-S6), along with all of the country-level population-weighted exposure data (mean,

278 95% uncertainty interval) for both PM_{2.5} and ozone for 1990, 1995, 2000, 2005, 2010 and 2013)
279 (File S1; Supporting Information). By way of example, Table 1 presents population-weighted
280 estimates for PM_{2.5} and ozone for 1990 and 2013 for the world's ten most populous countries.
281 Large proportional increases in mean population-weighted PM_{2.5} concentrations were apparent in
282 India, China, Brazil, Bangladesh, India, China and Pakistan, with decreases observed in the U.S.,
283 Indonesia, Russia, Japan, and Nigeria.

284 Between 1990 and 2013, decreases in population-weighted mean concentrations of PM_{2.5} were
285 evident in most of the high income countries (Figure 6a), in contrast to consistent increases in
286 South Asia (Figure 6b), much of Southeast Asia, and especially in China (Figure 6c). At the
287 country-level, the highest population-weighted mean concentration estimated for 2013 was
288 Mauritania (70 µg/m³), followed by China (55 µg/m³), Saudi Arabia (54 µg/m³), Kuwait (49
289 µg/m³), Bangladesh (48 µg/m³), India (47 µg/m³), Pakistan and Nepal (46 µg/m³). The lowest
290 country-level population-weighted estimates were for several Pacific and Caribbean island
291 nations, Australia and Norway (≤ 6 µg/m³). Population-weighted ozone levels also increased
292 throughout most of the most heavily populated countries from 1990 - 2013, although to a lesser
293 degree than seen for PM_{2.5}. There were modest decreases in population-weighted ozone levels in
294 the U.S., Mexico and Canada as well as parts of Europe and several countries in southeast Asia
295 (Indonesia, Malaysia, Singapore) (Table S1; Supporting Information).

296 We also compared estimates using the updated methodology described in this manuscript for the
297 year 2010 to those reported previously from GBD 2010² for the same year (Figure S7;
298 Supporting Information). This is a comparison of methodology, in contrast to the description of
299 temporal changes described above. Our updated estimates resulted in lower levels in areas of
300 North Africa, the Middle East and the Gobi Desert, all areas that were impacted by high levels of

301 windblown mineral dust. Slightly higher levels were estimated with the updated methodology in
302 Brazil and elsewhere in South America with noticeably higher levels in India, Pakistan and
303 Bangladesh. Somewhat lower levels were also estimated for some areas of eastern China. These
304 differences may be due to additional temporal coverage that is incorporated into the current
305 satellite-based and ground measurements. In North Africa the lower levels reflect changes in
306 mineral dust emissions that were driven by changes in local meteorology, and the higher levels in
307 India, Bangladesh and Pakistan likely reflect increases in emissions that may not have been
308 represented in the earlier methodology that extrapolated 2005 estimates to 2010. In China, the
309 somewhat lower levels were likely affected by the inclusion in the calibration of substantially
310 more ground measurements of high concentrations from China which tend to reduce the slope of
311 the calibration function (see Figure S2; Supporting Information).

312 At the country-level, population-weighted mean estimates for PM_{2.5} for the year 2010 were very
313 similar for most countries between those estimated for GBD 2010 and GBD 2013, and
314 discrepancies reflect the same patterns described above. Estimates for China were noticeably
315 lower for GBD 2013 (54.8 µg/m³) compared to GBD 2010 (72.6 µg/m³), as were several
316 countries with high contributions from windblown mineral dust (Saudi Arabia: 53.8 vs 61.7
317 µg/m³; Qatar: 40.1 vs 69.0 µg/m³; United Arab Emirates: 40.9 vs 79.5 µg/m³ for GBD 2013 vs
318 GBD 2010, respectively). Higher levels were estimated in GBD 2013 for countries in South Asia
319 (India: 43.4 vs 32.0; Bangladesh: 45.7 vs 31.1 6; Pakistan: 43.4 vs 38.1; Nepal: 41.5 vs 32.7
320 µg/m³ for GBD 2013 vs GBD 2010, respectively).

321

322 **Discussion**

323 We have extended previous global estimates of long-term average exposure to PM_{2.5} and ozone
324 at 0.1 x 0.1° resolution to support the Global Burden of Disease 2013. Specifically, we applied
325 improved satellite-based estimates that also incorporated additional information on temporal
326 trends, as well as chemical transport model simulations incorporating internally consistent
327 emissions trends from 1990 – 2013. Further, we have incorporated a substantially larger number
328 of available surface measurements of PM_{2.5} to calibrate the estimates based on satellite retrievals
329 and chemical transport model simulations. Given the increasing emphasis with in the Global
330 Burden of Disease on country-level (and sub-country) reporting, we also provided population-
331 weighted estimates of exposure to PM_{2.5} and ozone for 188 different countries for the years 1990,
332 1995, 2000, 2005, 2010 and 2013. As such, these data represent one of the most extensive
333 collections of global air pollution concentration estimates produced to date. Given the advances
334 in our methodology used to develop these estimates, compared to those previously reported², we
335 consider these estimates to be more accurate.

336
337 Although these estimates incorporated recent advances in satellite-based estimation, newly
338 developed emissions inventories and substantially more ground measurements, they are not
339 without limitations. Given the need to produce similar estimates in future years in support of
340 regular updates to the Global Burden of Disease³⁰ and other assessments, we anticipate further
341 enhancements to the methodology to address these limitations. Specifically, we note that there is
342 still poor agreement between these estimates and ground-based measurements in some locations,
343 notably in parts of South America (e.g. Chile), southern Poland and Turkey, and in specific
344 urban areas with high levels of ambient PM_{2.5} such as Ulaanbaatar, Mongolia (Figure S8;
345 Supporting Information) where ground measurements were underestimated by our approach.

346 The same underestimation of ground level measurements in southern Poland and Ulaanbaatar
347 was identified by van Donkelaar et al, who suggested that higher wintertime (and in the case of
348 Ulaanbaatar also nighttime) emissions when satellite retrievals are more limited due to more
349 frequent winter cloud cover (or unavailable at night) are likely to be responsible¹⁴. A similar
350 phenomenon may also be contributing to poor agreement in Chile where winter, nighttime wood
351 burning is a major contributor to elevated PM_{2.5} concentrations^{31,32}. We do note however, that
352 these same discrepancies and general underestimation of ground measurements in specific
353 locations are not restricted to the satellite-based estimates as they are also evident in TM5-
354 FASST simulations suggesting that both approaches may fail to accurately estimate ground-level
355 PM_{2.5} in relatively small areas having very high levels.

356
357 In addition, we used available PM₁₀ ground measurements to estimate PM_{2.5} concentrations in
358 locations where PM_{2.5} measurements were not available. Our use of PM_{2.5}:PM₁₀ ratios for the
359 measurement calibration dataset represents a balance between measurement specificity and
360 spatial representativeness of the ground measurements. For example in North Africa and the
361 Middle East, South Asia, and high-income Asia Pacific countries, less than 20% of available
362 ground measurements were of PM_{2.5}. Despite increases in the number of available PM_{2.5}
363 measurements used in our calibration (4073 in this analysis compared to 679 in that reported
364 previously²), more than 50% of the ground measurements that were used were estimated from
365 PM₁₀ measurements. Given the importance of these estimates in the calibration, we placed
366 additional importance on using location-specific PM_{2.5}:PM₁₀ ratios to estimate PM_{2.5}
367 concentrations, for example using ratios from measurements within 50km in 30% of cases and
368 in-country ratios for an additional 23% of cases. Further, our regression calibration included a

369 term to account for the use of direct vs estimated PM_{2.5} measurements. Van Donkelaar et al.,
370 using the same satellite-derived estimates included here, reported 58%, 53% and 65% of
371 explained variability in ground measurements of PM_{2.5} in North America, Europe and elsewhere,
372 respectively¹⁴. In comparison, our candidate simple regression model, which treated directly
373 measured and estimated ground PM_{2.5} measurements equally, explained 60% of variability in
374 ground measurements, while the (advanced) calibration model that was ultimately used
375 explained slightly more variability (64%). Overall, there is a need for additional PM_{2.5}
376 measurements and greater global coverage. The establishment of a new global network to
377 address these shortcomings and to improve the capability of satellite-based estimates of global
378 particulate matter levels offers the promise of enhanced accuracy and representativeness³³. The
379 need for additional air pollution measurements was also specifically highlighted in the recent
380 World Health Assembly Resolution on Air Pollution³⁴.

381
382 High levels of uncertainty in our estimates exist in regions of elevated windblown mineral dust.
383 The latter is partially driven by TM5-FASST use of standard dust contributions that do not align
384 with a specific year and the temporally variable levels of resuspended mineral dust in affected
385 regions. As we observed variability between regions in the function used to calibrate the fused
386 estimates ground measurements, there is a need to improve the incorporation of measurement
387 information. For example, in future work we aim to make use of the increasing number of
388 surface measurements, especially those in China, and to implement advanced approaches to
389 incorporate ground measurements and other information more directly into the estimates. Future
390 availability of additional ground measurements may also increase the feasibility of allowing
391 spatially varying calibration functions. This might be achieved by geographically weighted

392 regression³⁵ or hierarchical modelling. For the latter, calibration models for different regions may
393 include a global calibration together with regional random effects. Such models sit naturally
394 within a Bayesian framework. Recent advances in computational methods for inference, for
395 example those based on Integrated Nested Laplace Approximations^{36,37}, have increased the
396 feasibility of implementing such complex models in this setting. Harmonization of measurement
397 approaches between jurisdictions would also be beneficial.

398 Because we estimated year 2013 concentrations based upon year 2010 concentrations and trends
399 in satellite-based estimates from 2010 to 2011, differences between estimates for 2010 and 2013
400 from this analysis may be overly influenced by short-term variability in meteorology rather than
401 longer-term trends in emissions, the latter being more stable over the 5-year periods included in
402 our estimates. However, as noted in Methods, the annual satellite-based estimates are 3-year
403 moving averages, centered on the year of interest (for example 2010 includes retrievals from
404 2009-2011) which should partially mitigate this instability.

405 The updated global exposure estimates presented here represent a further advance in
406 characterizing global population exposure to ambient air pollution for use in burden of disease
407 assessment and other impact analyses. The global coverage allows for estimation of
408 concentrations in areas without extensive ground monitoring, including for example, rural areas
409 with large emissions from household use of solid fuels⁶. Like our previous GBD 2010 estimates,
410 these are based on PM_{2.5} mass concentrations. Although there is considerable interest in, and
411 active research concerning, the effects of the myriad constituents of ambient air pollution, ozone
412 and PM_{2.5} mass concentrations remain the most robust and consistent indicators of health-
413 damaging air pollution from combustion and other major sources^{38,39}. Use of these estimates in
414 combination with chemical transport model simulations can provide information on sector-

415 specific contributions to ambient concentrations and disease burden to inform air quality
416 management⁴⁻⁷. Improvements in the quality of these estimates and the application of a
417 consistent methodology to evaluate temporal trends in exposure over a 23 year period should
418 inform the choice of air quality management strategies and other approaches to mitigate the
419 health impacts of air pollution exposure. Accordingly, we are committed to making these
420 estimates available for others to use and have provided the associated files of country-level
421 population weighted (File S1) and gridded estimates (linked to population data and urbanicity
422 indicators, File S2) and a data dictionary (File S3) in the Supporting Information. Given the
423 evidence indicating the importance of ambient air pollution to global disease burden^{1,8}, we
424 anticipate a need for regular updating and improving of these estimates and their use in policy
425 assessments and comparative analyses.

426

427

428 **Acknowledgements**

429 We thank the following Global Burden of Disease Collaborators for comments on an earlier draft
430 of the manuscript: Kim Yun Jin, Samath Dharmaratne, Maysaa El Sayed Zaki, Jost Jonas,
431 Farshad Pourmalek, Arindam Basu, Michelle Bell, Yousef Khader, Eun-Kee Park, Kingsley
432 Nnnanna Ukwaja, Mark Nieuwenhuijsen, Ivy Shiue, George Thurston, Yuchiro Yano, Dean
433 Hosgood, Awoke Misganaw, Jiang Guohong, Yohannes Adama Melaku, Semaw Ferede Abera,
434 Dietrich Plaß, Sung Kim, Ted Miller, Scott Weichenthal, Elisabete Weiderpass, Ricky Leung,
435 Yoshihiro Kokubo, Hwasin Shin.

436

437

	1990	2013	%	1990	2013	%
Country	PM_{2.5}	PM_{2.5}	Change	Ozone	Ozone	Change
China	39.3	54.3	38.0	57.0	64.5	13.2
India	30.2	46.7	54.3	61.5	74.0	20.2
United States	16.4	10.7	-34.5	70.3	67.0	-4.7
Indonesia	21.0	14.8	-29.7	47.3	39.6	-16.1
Brazil	9.7	16.5	70.4	43.4	51.0	17.3
Pakistan	36.5	46.2	26.3	59.0	68.8	16.5
Nigeria	31.0	29.5	-4.7	66.3	67.5	1.9
Bangladesh	29.9	48.3	61.6	59.4	72.0	21.3
Russia	19.7	14.2	-27.6	48.6	48.3	-0.6
Japan	19.4	16.0	-17.5	56.8	60.5	6.7

438

439 **Table 1.** 1990, 2013 and percent change since 1990 in annual average PM_{2.5} (µg/m³) and
440 seasonal mean 1 hour daily maximum ozone (ppb) concentrations for the world's ten most
441 populous countries.

442

443 **References**

- 444 (1) Lim, S. S.; Vos, T.; Flaxman, A. D.; Danaei, G.; Shibuya, K.; Adair-Rohani, H.; Amann,
 445 M.; Anderson, H. R.; Andrews, K. G.; Aryee, M.; et al. A comparative risk assessment of
 446 burden of disease and injury attributable to 67 risk factors and risk factor clusters in 21
 447 regions, 1990-2010: a systematic analysis for the Global Burden of Disease Study 2010.
 448 *Lancet* **2012**, *380* (9859), 2224–2260.
- 449 (2) Brauer, M.; Amann, M.; Burnett, R. T.; Cohen, A.; Dentener, F.; Ezzati, M.; Henderson,
 450 S. B.; Krzyzanowski, M.; Martin, R. V; Van Dingenen, R.; et al. Exposure assessment for
 451 estimation of the global burden of disease attributable to outdoor air pollution. *Environ.*
 452 *Sci. Technol.* **2012**, *46* (2), 652–660.
- 453 (3) Li, Y.; Henze, D.; Jack, D.; Kinney, P. The influence of air quality model resolution on
 454 health impact assessment for fine particulate matter and its components. *Air Qual. Atmos.*
 455 *Heal.* **2015**, 1–18.
- 456 (4) Bhalla, K.; Shotten, M.; Cohen, A.; Brauer, M.; Shahraz, S.; Burnett, R.; Leach-Kemon,
 457 K.; Freedman, G.; Murray, C. J. L. *Transport for health : the global burden of disease*
 458 *from motorized road transport*; World Bank Group: Washington, DC, 2014.
- 459 (5) Minjares, S. E. C. and R. S. and J. J. W. and M. Z. and R. Estimating source-attributable
 460 health impacts of ambient fine particulate matter exposure: global premature mortality
 461 from surface transportation emissions in 2005. *Environ. Res. Lett.* **2014**, *9* (10), 104009.
- 462 (6) Chafe, Z. A.; Brauer, M.; Klimont, Z.; Van Dingenen, R.; Mehta, S.; Rao, S.; Riahi, K.;
 463 Dentener, F.; Smith, K. R. Household cooking with solid fuels contributes to ambient
 464 PM_{2.5} air pollution and the burden of disease. *Environ. Health Perspect.* **2014**, *122* (12),
 465 1314–1320.
- 466 (7) *Residential heating with wood and coal: health impacts and policy options in Europe and*
 467 *North America*; World Health Organization, Regional Office for Europe: Copenhagen,
 468 Denmark, 2015;
 469 [http://www.euro.who.int/__data/assets/pdf_file/0009/271836/ResidentialHeatingWoodCo](http://www.euro.who.int/__data/assets/pdf_file/0009/271836/ResidentialHeatingWoodCoalHealthImpacts.pdf)
 470 [alHealthImpacts.pdf](http://www.euro.who.int/__data/assets/pdf_file/0009/271836/ResidentialHeatingWoodCoalHealthImpacts.pdf)
- 471 (8) WHO | Mortality from ambient air pollution.
 472 http://www.who.int/gho/phe/outdoor_air_pollution/burden/en/ (accessed Jul 22, 2015)
- 473 (9) *World Development Indicators 2015*; The World Bank, 2015;
 474 <https://openknowledge.worldbank.org/handle/10986/21634>
- 475 (10) Cropper, M.L.; Khanna, S. *How Should the World Bank Estimate Air Pollution Damages?*
 476 *RFF Discussion Paper 14-30.* **2014** . [http://www.rff.org/RFF/Documents/RFF-DP-14-](http://www.rff.org/RFF/Documents/RFF-DP-14-30.pdf)
 477 [30.pdf](http://www.rff.org/RFF/Documents/RFF-DP-14-30.pdf)

- 478 (11) US EPA. Environmental Benefits Mapping and Analysis Program - Community Edition
 479 (BenMAP-CE). <http://www2.epa.gov/benmap> (accessed Jul 22, 2015)
- 480 (12) Loomis, D.; Grosse, Y.; Lauby-Secretan, B.; El Ghissassi, F.; Bouvard, V.; Benbrahim-
 481 Tallaa, L.; Guha, N.; Baan, R.; Mattock, H.; Straif, K. The carcinogenicity of outdoor air
 482 pollution. *Lancet. Oncol.* **2013**, *14* (13), 1262–1263.
- 483 (13) Global, regional, and national age–sex specific all-cause and cause-specific mortality for
 484 240 causes of death, 1990–2013: a systematic analysis for the Global Burden of Disease
 485 Study 2013. *Lancet* **2014**, *385* (9963), 117–171.
- 486 (14) Van Donkelaar, A.; Martin, R. V; Brauer, M.; Boys, B. L. Use of satellite observations for
 487 long-term exposure assessment of global concentrations of fine particulate matter.
 488 *Environ. Health Perspect.* **2015**, *123* (2), 135–143.
- 489 (15) Van Donkelaar, A.; Martin, R. V; Brauer, M.; Kahn, R.; Levy, R.; Verduzco, C.;
 490 Villeneuve, P. J. Global estimates of ambient fine particulate matter concentrations from
 491 satellite-based aerosol optical depth: development and application. *Environ. Health*
 492 *Perspect.* **2010**, *118* (6), 847–855.
- 493 (16) Huijnen, V.; Williams, J.; van Weele, M.; van Noije, T.; Krol, M.; Dentener, F.; Segers,
 494 A.; Houweling, S.; Peters, W.; de Laat, J.; et al. The global chemistry transport model
 495 TM5: description and evaluation of the tropospheric chemistry version 3.0. *Geosci. Model*
 496 *Dev.* **2010**, *3* (2), 445–473.
- 497 (17) Bey, I.; Jacob, D. J.; Yantosca, R. M.; Logan, J. A.; Field, B. D.; Fiore, A. M.; Li, Q.; Liu,
 498 H. Y.; Mickley, L. J.; Schultz, M. G. Global modeling of tropospheric chemistry with
 499 assimilated meteorology: Model description and evaluation. *J. Geophys. Res.* **2001**, *106*
 500 (D19), 23073.
- 501 (18) Levy, R. C.; Remer, L. A.; Mattoo, S.; Vermote, E. F.; Kaufman, Y. J. Second-generation
 502 operational algorithm: Retrieval of aerosol properties over land from inversion of
 503 Moderate Resolution Imaging Spectroradiometer spectral reflectance. *J. Geophys. Res.*
 504 *Atmos.* **2007**, *112* (D13), n/a – n/a.
- 505 (19) J., D. D.; H., B. B.; Roger, D.; NADINE, G.; Jiannan, H.; Yufang, J.; A., K. R.; Yuri, K.;
 506 Norman, L.; Jan-Peter, M.; et al. *The Value of Multiangle Measurements for Retrieving*
 507 *Structurally and Radiatively Consistent Properties of Clouds, Aerosols, and Surfaces*;
 508 Elsevier, 2005.
- 509 (20) *Satellite Aerosol Remote Sensing over Land*; Kokhanovsky, A. A., de Leeuw, G., Eds.;
 510 Springer Berlin Heidelberg: Berlin, Heidelberg, 2009.
- 511 (21) Hsu, N. C.; Jeong, M.-J.; Bettenhausen, C.; Sayer, A. M.; Hansell, R.; Seftor, C. S.;
 512 Huang, J.; Tsay, S.-C. Enhanced Deep Blue aerosol retrieval algorithm: The second
 513 generation. *J. Geophys. Res. Atmos.* **2013**, *118* (16), 9296–9315.

- 514 (22) Winker, D. M.; Pelon, J. R.; McCormick, M. P. <title>The CALIPSO mission: spaceborne
515 lidar for observation of aerosols and clouds</title>. In *Third International Asia-Pacific*
516 *Environmental Remote Sensing Remote Sensing of the Atmosphere, Ocean, Environment,*
517 *and Space*; Singh, U. N., Itabe, T., Liu, Z., Eds.; International Society for Optics and
518 Photonics, 2003; pp 1–11.
- 519 (23) Janssens-Maenhout, G.; Dentener, F.; Aardenne, J. Van; Monni, S.; Pagliari, V.;
520 Orlandini, L.; Klimont, Z.; Kurokawa, J.; Akimoto, H.; Ohara, T.; et al. *EDGAR-HTAP: A*
521 *Harmonized Gridded Air Pollution Emission Dataset Based on National Inventories*;
522 Publications Office, 2011.
- 523 (24) Boys, B. L.; Martin, R. V; van Donkelaar, A.; MacDonell, R. J.; Hsu, N. C.; Cooper, M.
524 J.; Yantosca, R. M.; Lu, Z.; Streets, D. G.; Zhang, Q.; et al. Fifteen-year global time series
525 of satellite-derived fine particulate matter. *Environ. Sci. Technol.* **2014**, *48* (19), 11109–
526 11118.
- 527 (25) Van Dingenen, R.; Leita, J.; Dentener, F. A multi-metric global source-receptor model
528 for integrated impact assessment of climate and air quality policy scenarios. *EGU Gen.*
529 *Assem. 2014* **2014**.
- 530 (26) *Report on spatial emissions downscaling and concentrations for health impacts*
531 *assessment*. International Institute for Applied Systems Analysis (IIASA). 2013.
532 http://www.feem-project.net/limits/docs/limits_d4-2_iiasa.pdf
- 533 (27) Gridded Population of the World (GPW), v3 | SEDAC
534 <http://sedac.ciesin.columbia.edu/data/collection/gpw-v3> (accessed Jul 22, 2015).
- 535 (28) Brauer, M.; Amann, M.; Burnett, R. T.; Cohen, A.; Dentener, F.; Ezzati, M.; Henderson,
536 S. B.; Krzyzanowski, M.; Martin, R. V; Van Dingenen, R.; et al. Exposure Assessment for
537 Estimation of the Global Burden of Disease Attributable to Outdoor Air Pollution.
538 *Environ. Sci. Technol.* **2012**, *46* (2), 652–660.
- 539 (29) Lall, R.; Kendall, M.; Ito, K.; Thurston, G. D. Estimation of historical annual PM2.5
540 exposures for health effects assessment. *Atmos. Environ.* **2004**, *38* (31), 5217–5226.
- 541 (30) *Protocol for the Global Burden of Diseases, Injuries, and Risk Factors Study (GBD)*;
542 Institute for Health Metrics and Evaluation: Seattle, USA; 2015.
543 http://www.healthdata.org/sites/default/files/files/Projects/GBD/GBD_Protocol.pdf
- 544 (31) Sanhueza, P. A.; Torreblanca, M. A.; Diaz-Robles, L. A.; Schiappacasse, L. N.; Silva, M.
545 P.; Astete, T. D. Particulate Air Pollution and Health Effects for Cardiovascular and
546 Respiratory Causes in Temuco, Chile: A Wood-Smoke-Polluted Urban Area. *J. Air Waste*
547 *Manage. Assoc.* **2009**, *59* (12), 1481–1488.

- 548 (32) Kavouras, I. G.; Koutrakis, P.; Cereceda-Balic, F.; Oyola, P. Source Apportionment of
549 PM 10 and PM 25 in Five Chilean Cities Using Factor Analysis. *J. Air Waste Manage.*
550 *Assoc.* **2001**, *51* (3), 451–464.
- 551 (33) Snider, G.; Weagle, C. L.; Martin, R. V.; van Donkelaar, A.; Conrad, K.; Cunningham, D.;
552 Gordon, C.; Zwicker, M.; Akoshile, C.; Artaxo, P.; et al. SPARTAN: a global network to
553 evaluate and enhance satellite-based estimates of ground-level particulate matter for
554 global health applications. *Atmos. Meas. Tech.* **2015**, *8* (1), 505–521.
- 555 (34) The Lancet. Air pollution at the forefront of global health. *Lancet* **2015**, 385 (9984), 2224.
- 556 (35) Hu, X.; Waller, L. A.; Al-Hamdan, M. Z.; Crosson, W. L.; Estes, M. G.; Estes, S. M.;
557 Quattrochi, D. A.; Sarnat, J. A.; Liu, Y. Estimating ground-level PM(2.5) concentrations
558 in the southeastern U.S. using geographically weighted regression. *Environ. Res.* **2013**,
559 *121*, 1–10.
- 560 (36) Shaddick, G.; Zidek, J. V. A case study in preferential sampling: Long term monitoring of
561 air pollution in the UK. *Spat. Stat.* **2014**, *9*, 51–65.
- 562 (37) Cameletti, M.; Lindgren, F.; Simpson, D.; Rue, H. Spatio-temporal modeling of
563 particulate matter concentration through the SPDE approach. *AStA Adv. Stat. Anal.* **2012**,
564 *97* (2), 109–131.
- 565 (38) *Review of evidence on health aspects of air pollution – REVIHAAP project: final technical*
566 *report*. World Health Organization, Regional Office for Europe: Copenhagen, Denmark,
567 2013; [http://www.euro.who.int/__data/assets/pdf_file/0004/193108/REVIHAAP-Final-](http://www.euro.who.int/__data/assets/pdf_file/0004/193108/REVIHAAP-Final-technical-report-final-version.pdf)
568 [technical-report-final-version.pdf](http://www.euro.who.int/__data/assets/pdf_file/0004/193108/REVIHAAP-Final-technical-report-final-version.pdf)
- 569 (39) *Health risks of air pollution in Europe – HRAPIE project. Recommendations for*
570 *concentration–response functions for cost–benefit analysis of particulate matter, ozone*
571 *and nitrogen dioxide*. World Health Organization, Regional Office for Europe:
572 Copenhagen, Denmark, 2013;
573 [http://www.euro.who.int/__data/assets/pdf_file/0006/238956/Health-risks-of-air-](http://www.euro.who.int/__data/assets/pdf_file/0006/238956/Health-risks-of-air-pollution-in-Europe-HRAPIE-project,-Recommendations-for-concentrationresponse-functions-for-costbenefit-analysis-of-particulate-matter,-ozone-and-nitrogen-dioxide.pdf)
574 [pollution-in-Europe-HRAPIE-project,-Recommendations-for-concentrationresponse-](http://www.euro.who.int/__data/assets/pdf_file/0006/238956/Health-risks-of-air-pollution-in-Europe-HRAPIE-project,-Recommendations-for-concentrationresponse-functions-for-costbenefit-analysis-of-particulate-matter,-ozone-and-nitrogen-dioxide.pdf)
575 [functions-for-costbenefit-analysis-of-particulate-matter,-ozone-and-nitrogen-dioxide.pdf](http://www.euro.who.int/__data/assets/pdf_file/0006/238956/Health-risks-of-air-pollution-in-Europe-HRAPIE-project,-Recommendations-for-concentrationresponse-functions-for-costbenefit-analysis-of-particulate-matter,-ozone-and-nitrogen-dioxide.pdf)
- 576